Expanded View Figures

Figure EV1. Tau phosphorylated in cells can undergo LLPS.

A Example FRAP images of GFP-tau441 droplet (green circle and arrowhead) in primary neurons. Recovery after photobleaching event appears rapid but incomplete.

B FRAP of tau aggregates in HEK TauRDP301S-CFP/YFP cells shows no recovery after photobleaching of the aggregates that have been initiated with brain lysate (5 μg/μl total protein) from human tauP301L transgenic mice (rTg4510 line). Insets show example images taken before bleaching and at t = 0 and 300 s. FRAP parameters were the same as in (A, C). Graph represents mean ± s.e.m. of n = 3 aggregates.

C FRAP of GFP-PolyQ aggregates that formed in primary cortical mouse neurons after overexpression for 24 h. PolyQ aggregates show no recovery after photobleaching. Insets show example images taken before bleaching and at t = 0 and 300 s. FRAP parameters were the same as in (A, B). Graph represents mean ± s.e.m. of n = 4 aggregates.

D Example FRAP experiment for GFP-tau441 expressed in primary cortical neurons. Cytosolic soluble GFP-tau441 shows rapid and complete recovery, whereas microtubule-bound GFP-tau441 in a neighboring cell recovers slightly slower. FRAP parameters were the same as in (A– C).

E Expression of AAV8 Dendra2-tau441 in the cortex of wild-type mice allows the visualization of droplet-like tau in cortical neuronal cell bodies (1–3) and processes (4–6) *in vivo* by two-photon microscopy. GFP expressing control neurons show a homogenous GFP distribution instead.

F Cell lysates from murine N2a cells and primary cortical mouse neurons (DIV7) expressing GFP-tau256 or GFP-tau441 were analyzed by Western blot for the content of human tau (Tau13) and phospho-tau using antibodies PHF-1 or a mix of p-Tau antibodies.

G Most abundant phosphorylation sites previously found in p-tau441 and deP-tau441 (*) by mass spectrometry (Mair *et al*, 2016). Most of these phospho-sites, for which specific antibodies were available, could be verified (red; blue = not detected) in the p-tau441 preparation used in this manuscript.

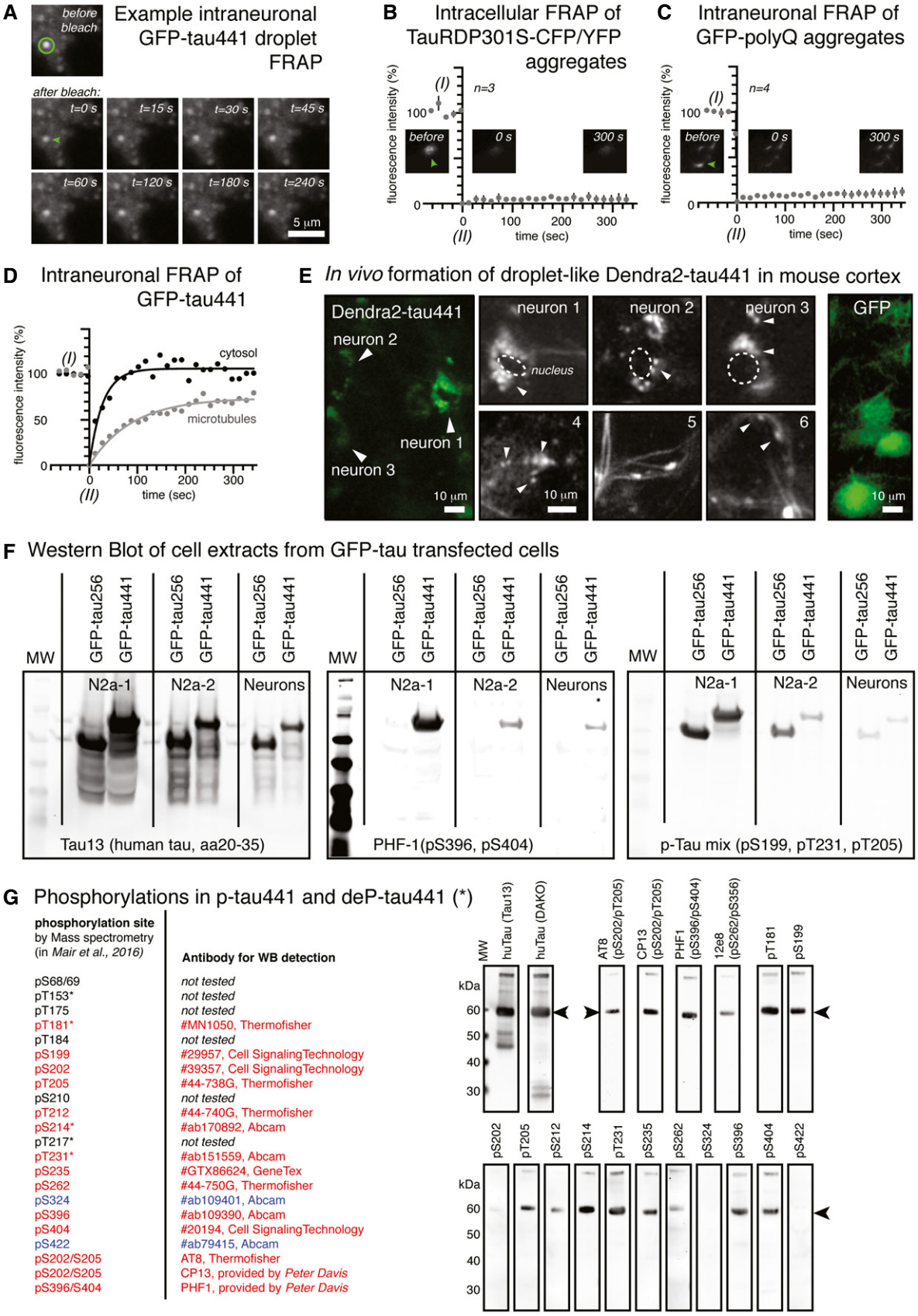
A
Example intraneuronal GFP-tau441 droplet FRAP
before bleach
after bleach:
t=0 s
t=15 s
t=30 s
t=45 s
t=60 s
t=120 s
t=180 s
t=240 s
5 µm
B
Intracellular FRAP of TauRDP301S-CFP/YFP aggregates
fluorescence intensity (%)
n=3
before
0 s
300 s
time (sec)
C
Intraneuronal FRAP of GFP-polyQ aggregates
n=4
D
Intraneuronal FRAP of GFP-tau441
cytosol
microtubules
E
In vivo formation of droplet-like Dendra2-tau441 in mouse cortex
Dendra2-tau441
neuron 1
neuron 2
neuron 3
nucleus
GFP
10 µm
F
Western Blot of cell extracts from GFP-tau transfected cells
MW
GFP-tau256
GFP-tau441
N2a-1
N2a-2
Neurons
Tau13 (human tau, aa20-35)
PHF-1(pS396, pS404)
p-Tau mix (pS199, pT231, pT205)
G
Phosphorylations in p-tau441 and deP-tau441 (*)
phosphorylation site by Mass spectrometry (in Mair et al., 2016)
Antibody for WB detection
pS68/69 not tested
pT153* not tested
pT175 not tested
pT181* #MN1050, Thermofisher
pT184 not tested
pS199 #29957, Cell SignalingTechnology
pS202 #39357, Cell SignalingTechnology
pT205 #44-738G, Thermofisher
pS210 not tested
pT212 #44-740G, Thermofisher
pS214* #ab170892, Abcam
pT217* not tested
pT231* #ab151559, Abcam
pS235 #GTX86624, GeneTex
pS262 #44-750G, Thermofisher
pS324 #ab109401, Abcam
pS396 #ab109390, Abcam
pS404 #20194, Cell SignalingTechnology
pS422 #ab79415, Abcam
pS202/S205 AT8, Thermofisher
pS202/S205 CP13, provided by Peter Davis
pS396/S404 PHF1, provided by Peter Davis
MW
huTau (Tau13)
huTau (DAKO)
AT8 (pS202/pT205)
CP13 (pS202/pT205)
PHF1 (pS396/pS404)
12e8 (pS262/pS356)
pT181
pS199
kDa
60
50
40
30
pS202
pT205
pS212
pS214
pT231
pS235
pS262
pS324
pS396
pS404
pS422

Figure EV1.

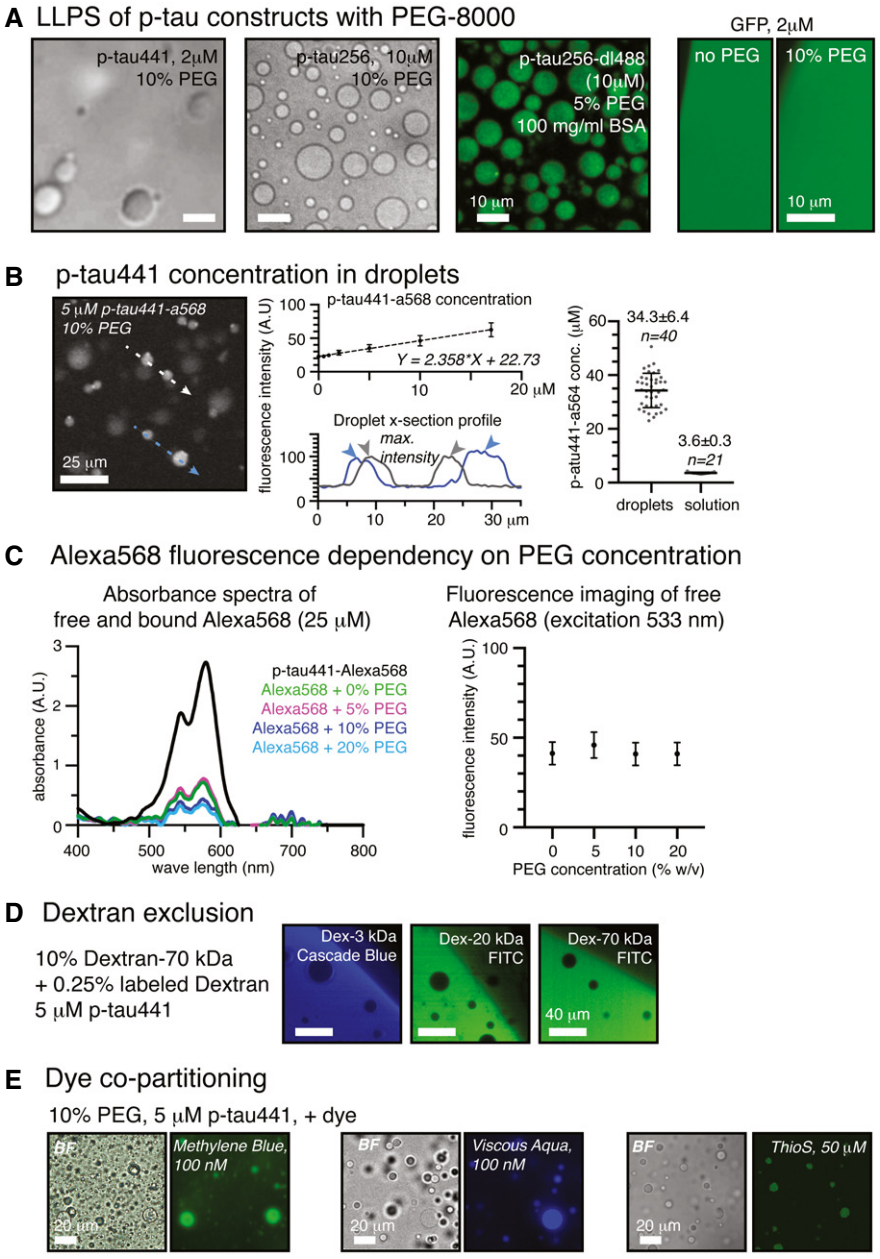

Figure EV2. *In vitro* phase separation of tau initiated by crowding agents.

A LLPS of p-tau441 and p-tau256 can also be initialized using crowding agent PEG-8000 or a combination of PEG-8000 with bovine serum albumin (BSA), whereas the soluble control protein GFP did not undergo LLPS in the presence of 10% PEG.

B We estimated the concentration of fluorescently labeled p-tau441-Alexa568 (10% PEG, 50 mM NaCl, 5 μM p-tau441-a568) in the droplets by confocal imaging (z = 2 μm) of 30-min-old droplets. The measured maximum droplet fluorescence intensity was calibrated against different concentrations of p-tau441-Alexa568 in solution without LLPS initiation (no PEG, 50 mM NaCl). Cross-sectional profile along the white arrow visualizes the intensity levels of droplets. The mean of the detected p-tau441-a568 concentration was 34.3 ± 6.4 μM in the droplets and 3.6 ± 0.3 μM in the solution phase. This value might be underestimating the actual tau concentration in the droplets because fluorophore:fluorophore quenching and other artifact resulting from the highly viscous and crowded environment in the droplets are not considered.

C Absorbance spectra of free and p-tau441 bound Alexa568 shows differences in the intensity but no shift in the wavelengths. The intensity of free Alexa568 dye imaged at 533 nm in confocal microscopy did not change with the amount of PEG in solution.

D By confocal imaging, the crowding agent dextran remains excluded from p-tau441 droplets initiated by adding 9% dextran-70 kDa and 1% of fluorescent dextrans of different molecular weights.

E The addition of methylene blue, viscous aqua, and ThioS, all dyes with affinity to hydrophobic protein areas, to freshly prepared p-tau441 droplets reveals the co-partitioning and retention of these dyes in the droplets. The fluorescence may be further enhanced by inhibition of free rotation of the dyes due to the higher droplet viscosity.

Data information: In right graphs of (B, C), data are represented as mean ± s.d.

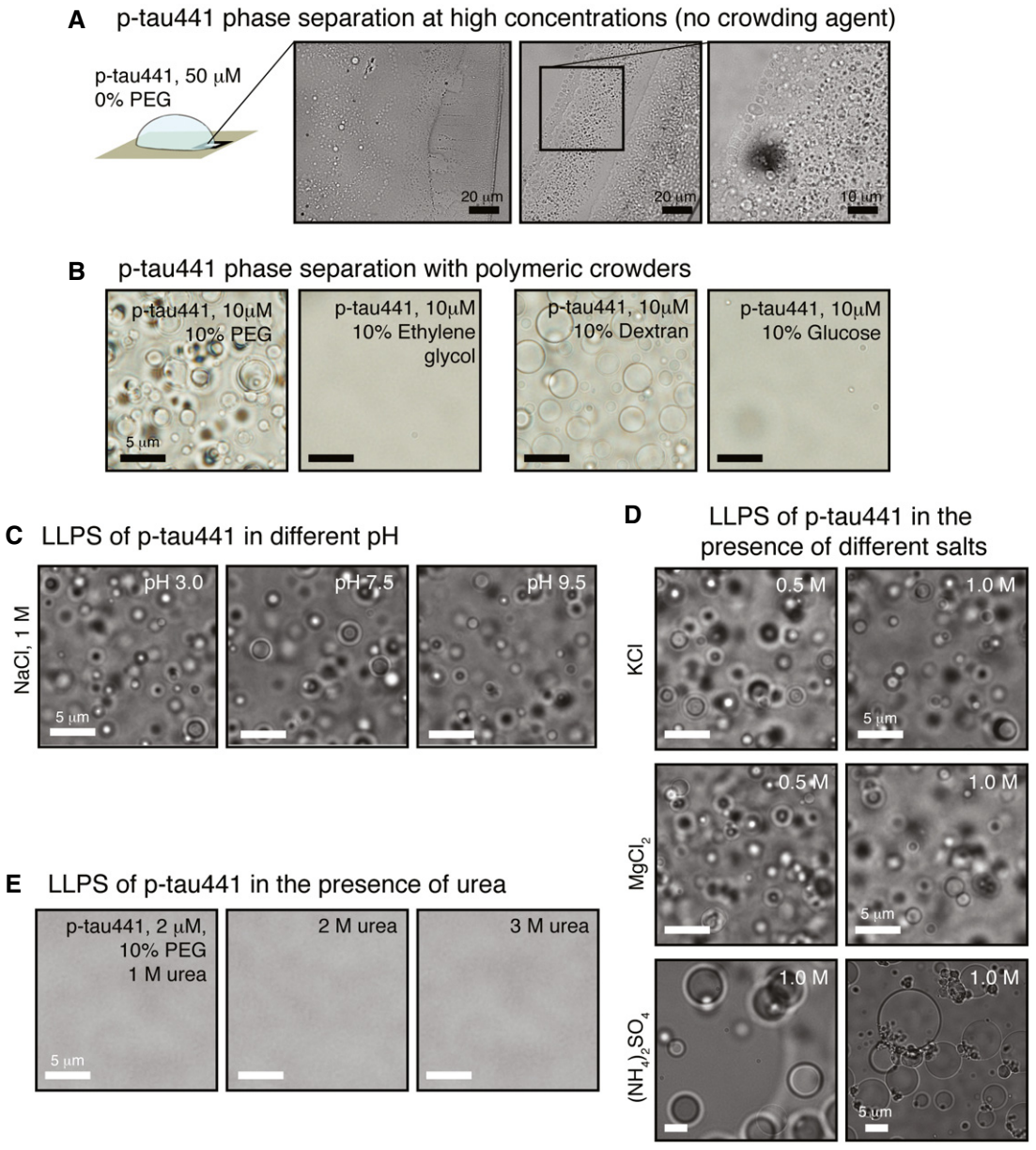

Figure EV3. ***In vitro*** **phase separation of tau initiated by crowding agents.**

A In solutions of high p-tau441 concentrations (50–100 μM), tau LLPS can occur even in absence of crowding agents, for example, due to protein supersaturation at the interface of a tau solution deposited on glass.

B Macromolecular crowding agents PEG-8000 and dextran-70 kDa, but not their monomeric building blocks ethylene glycol and glucose at the same percentage (% w/v), initiate p-tau441 LLPS, likely due to tau supersaturation caused by excluded volume effects. The very small droplet-like appearances in the images of p-tau441 with ethylene glycol and glucose are caused by imaging (lens) artifacts.

C LLPS of p-tau441 appeared independent on pH of the buffer used. The droplet amounts and sizes appeared very similar at pH 3.0, 7.5, and 9.5 (in the presence of 1 M NaCl).

D LLPS of p-tau441 in the presence of high salt concentrations. KCl and $MgCl_2$ did not change droplet size and amounts in the tested conditions (concentrations ≤ 1 M salt, 2.5 μM protein, 10% PEG, 3 h). Interestingly, the droplet size increased substantially in the presence of the cosmotropic salt $(NH_4)_2SO_4$.

E LLPS of p-tau441 was efficiently prevented in the presence of urea at concentrations between 1 and 3 M.

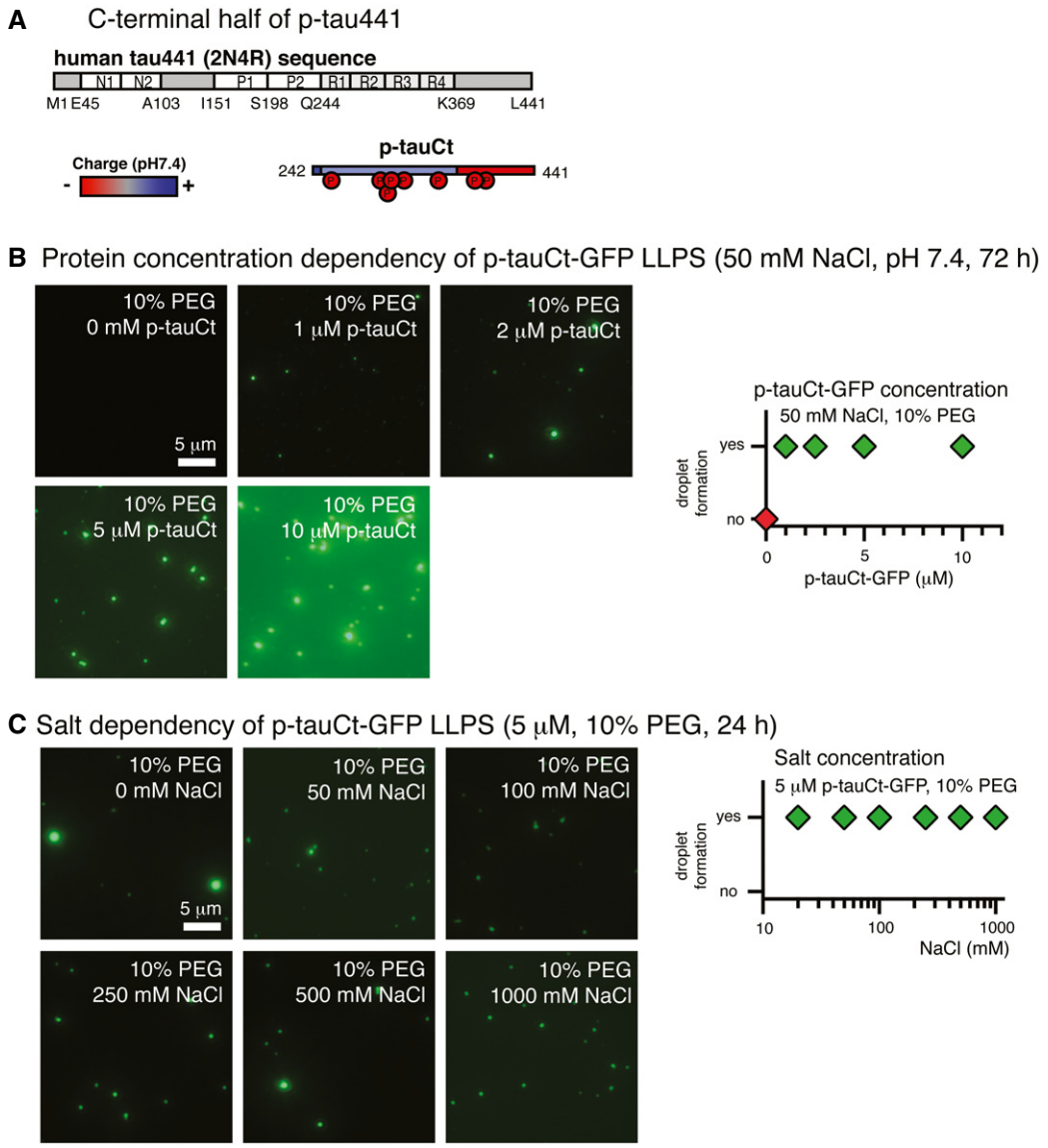

Figure EV4. LLPS of the phosphorylated C-terminal half of human tau441.

A The C-terminal half of tau441, tauCt (aa 242–441), fused to GFP was produced in SF9 cells to produce p-tauCt-GFP. Polypeptide charge of p-tauCt domains at pH 7.4 and approximated positions of phosphorylation sites are indicated.

B To evaluate the protein concentration dependency of p-tauCt LLPS, we added 10% PEG to different concentrations of p-tauCt-GFP and imaged and determined droplet formation after 3 h. p-tauCt-GFP formed very small droplets even at a protein concentration of 1 μM that seemed to increase in number with increasing protein concentration.

C We tested the salt dependency of p-tauCt-GFP droplet formation in a range of 0–1,000 mM NaCl. In all cases, p-tauCt-GFP formed similarly small droplets that did not increase in size over 72 h.

Figure EV5. LLPS of the phosphorylated N-terminal half of tau441.

A The N-terminal half of tau441, tau256 (aa 1–156), was produced in SF9 cells to produce p-tau256. Polypeptide charge domains at pH 7.4 and approximated positions of phosphorylation sites are indicated.

B LLPS of p-tau256 induced with Ficoll. Fluorescently labeled p-tau256-Alexa488 co-partitions into the droplets.

C p-tau256 droplets observed by transmission electron microscopy (TEM).

D Time-lapse imaging of p-tau256-Dylight488 droplet coalescence and mobility in solution. A small p-tau441-Dylight488 droplet (green arrowheads) fuses with a larger one and disperses its fluorophore content into the large droplet. Droplet fusion is shown also in Movie EV10.

E p-tau256-dl488 droplets (in buffer with 20% PEG) exhibit glass surface wetting properties characteristics for liquids. 3D-representation of confocal imaging *z*-stack of p-tau256-Dylight488 droplets attached to the glass surface in solution (left panel). After deposition on the glass surface, individual p-tau256 droplets can still move on the surface and fuse with each other (right panel). White lanes show the initial droplet position, white arrows indicate movement direction, and pink arrowheads indicate site of droplet fusion.

F Tau protein concentration, crowding agent concentration (% w/v), and buffer salt concentration (NaCl) conditions allowing (green squares) and preventing (red squares) for p-tau256 droplet formation (n = 3 per condition). Intracellular salt conditions (orange circle) also allowed for droplet formation. Presence of droplets was determined 3 h after.

G The addition of 10% 1,6-hexanediol seems to not change the amount of tau256 droplets initiated with 10% PEG.

H Western blots (reducing conditions = left panel; non-reducing conditions = right panel) of brain lysates from Alzheimer's disease (AD1–3) and control (C1–3) brains suggest the presence of N-terminal tau fragments (MW < 45 kDa) in healthy and diseased brains (full-length human tau has an apparent MW of ≈60 kDa). Size exclusion chromatography (SEC) of brain lysates performed in non-reducing conditions (right panel) shows that N-terminal tau fragments (MW < 45 kDa) occur in the low molecular weight (LMW) but not in the high molecular weight (HMW) SEC fraction of AD and control brain lysates. Blots were probed with antibody Tau13, which detects an epitope in the very N-terminus of human tau.

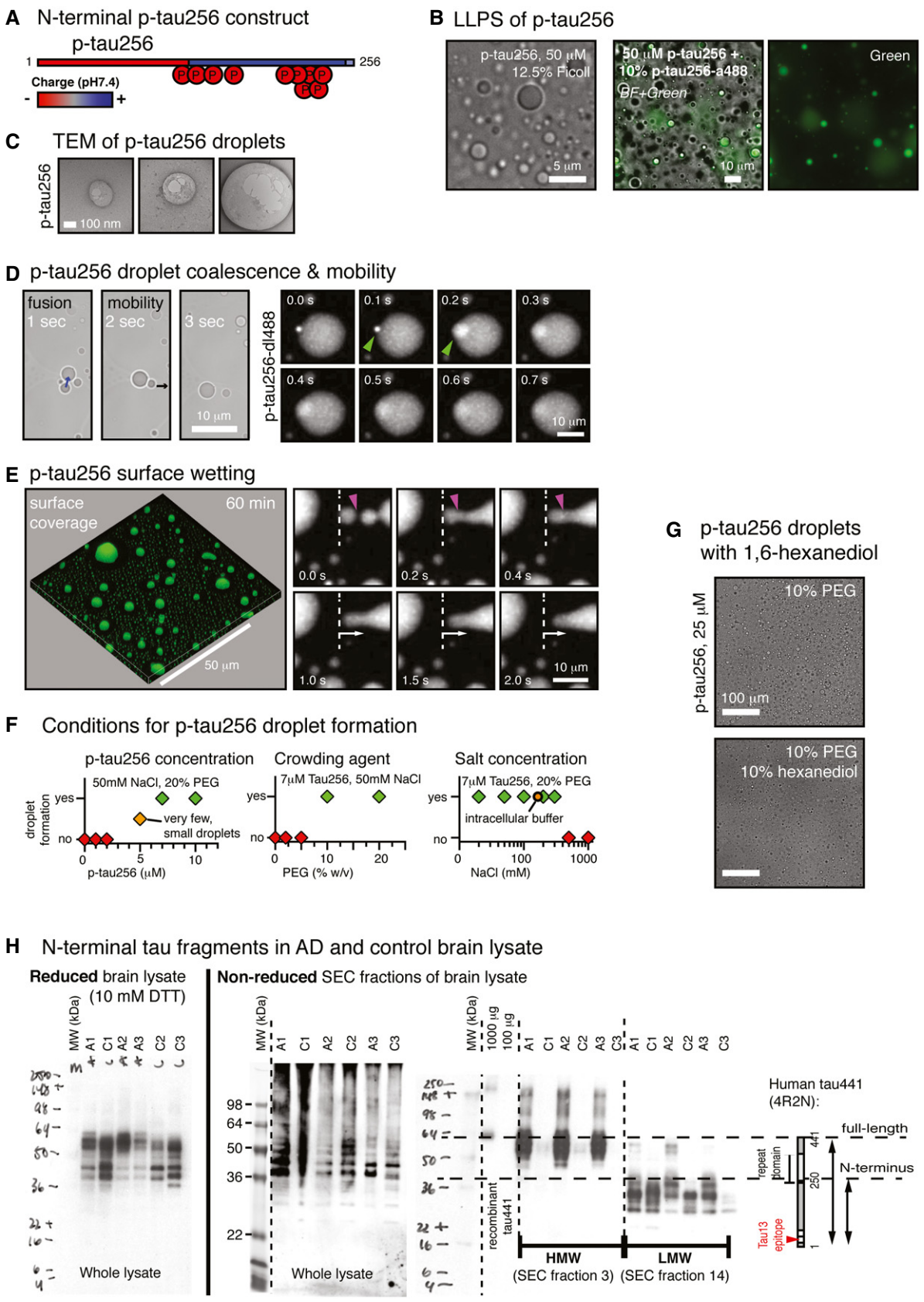
A N-terminal p-tau256 construct
p-tau256
1
256
Charge (pH7.4)
-
+
B LLPS of p-tau256
p-tau256, 50 µM
12.5% Ficoll
5 µm
50 µM p-tau256 +
10% p-tau256-a488
BF+Green
10 µm
Green
C TEM of p-tau256 droplets
p-tau256
100 nm
D p-tau256 droplet coalescence & mobility
fusion
1 sec
mobility
2 sec
3 sec
10 µm
p-tau256-dl488
0.0 s
0.1 s
0.2 s
0.3 s
0.4 s
0.5 s
0.6 s
0.7 s
10 µm
E p-tau256 surface wetting
surface
coverage
60 min
50 µm
0.0 s
0.2 s
0.4 s
1.0 s
1.5 s
2.0 s
10 µm
F Conditions for p-tau256 droplet formation
p-tau256 concentration
50mM NaCl, 20% PEG
very few,
small droplets
droplet formation
yes
no
p-tau256 (µM)
Crowding agent
7µM Tau256, 50mM NaCl
PEG (% w/v)
Salt concentration
7µM Tau256, 20% PEG
intracellular buffer
NaCl (mM)
G p-tau256 droplets
with 1,6-hexanediol
p-tau256, 25 µM
10% PEG
100 µm
10% PEG
10% hexanediol
H N-terminal tau fragments in AD and control brain lysate
Reduced brain lysate
(10 mM DTT)
Non-reduced SEC fractions of brain lysate
MW (kDa)
A1
C1
A2
C2
A3
C3
1000 µg
100 µg
Whole lysate
recombinant tau441
HMW
(SEC fraction 3)
LMW
(SEC fraction 14)
Human tau441
(4R2N):
full-length
N-terminus
repeat domain
Tau13 epitope

Figure EV5.

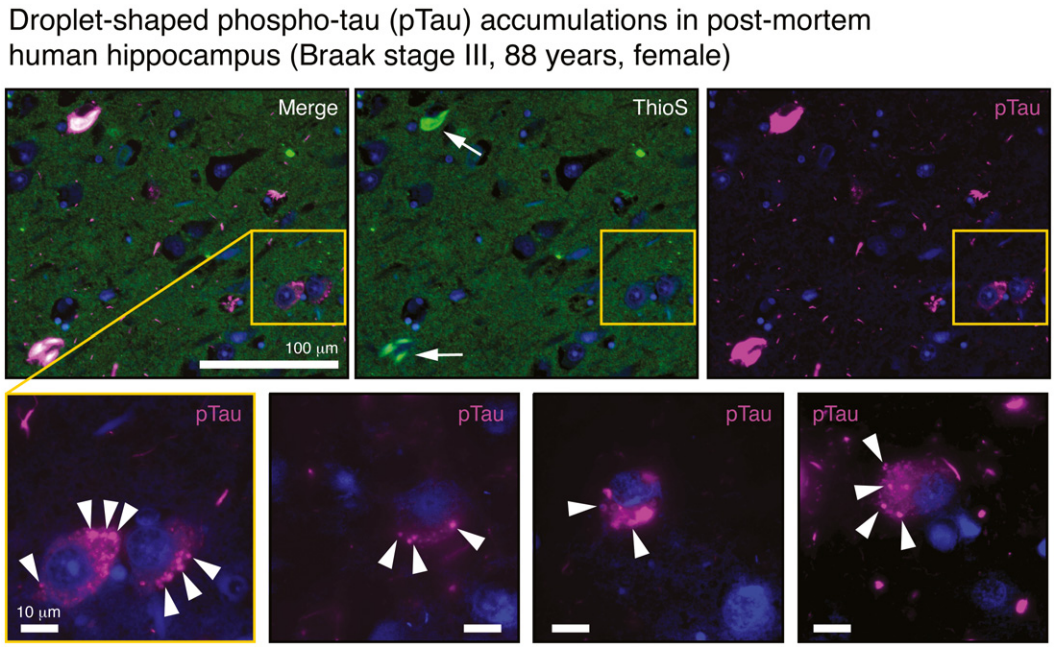

Figure EV6. Spherical tau accumulation in brain tissue of a mild AD case.

Paraffin-embedded brain slices from an old (88 years old, female) individual with mild AD (stage: Braak III) were immunofluorescently labeled with a mix of antibodies to detect phospho-tau (anti pT205, pS409, pT231, pS199, pT181) and with thioflavin-S (ThioS) to detect neurofibrillary tangles (NFTs; white arrows) consisting of aggregated tau. Droplet-like accumulations of phospho-tau (white arrowheads) could be found in cortical and hippocampal neuronal cell bodies without NFTs that have aberrant but only small amounts of phospho-tau in the cell body.